Annals of Emerging Technologies in Computing (AETiC)
Vol. 5, No. 4, 2021

Research Article

Towards 76-81 GHz Scalable Phase Shifting by Folded Dual-strip Shielded Coplanar Waveguide with Liquid Crystals

Jinfeng Li[1,*]

[1]Imperial College London, United Kingdom
jinfeng.li@imperial.ac.uk
*Correspondence: jinfeng.li@imperial.ac.uk

Received: 5th July 2021; Accepted: 26th September 2021; Published: 1st October 2021

Abstract: Unconventional folded shielded coplanar waveguide (FS-CPW) has yet to be fully investigated for tunable dielectrics-based applications. This work formulates designs of FS-CPW based on liquid crystals (LC) for electrically controlled 0-360° phase shifters, featuring a minimally redundant approach for reducing the LC volume and hence the costs for mass production. The design exhibits a few conceptual features that make it stand apart from others, noteworthy, the dual-strip structure with a simplified enclosure engraved that enables LC volume sharing between adjacent core lines. Insertion loss reduction by 0.77 dB and LC volume reduction by 1.62% per device are reported at 77 GHz, as compared with those of the conventional single-strip configuration. Based on the proof-of-concept results obtained for the novel dual-strip FS-CPW proposed, this work provides a springboard for follow-up investible propositions that will underpin the development of a phased array demonstrator.

Keywords: *computational electromagnetics; liquid crystal; meandered coplanar waveguide; passive microwave components; phase shifter; shielded coplanar waveguide; wireless communication; 77 GHz*

---

1. Introduction

Millimetre-wave (mm-Wave) mobile broadband terminals [1] are all the rage at the moment and becoming a prime need for wireless communication [2-4], detection [5], and sensing [6]. The technology realisation is increasingly relying on continuously tunable liquid crystals (LC) [7-9] based mm-Wave beam steering flat-panel [10] antennas array (static and fault-tolerant), in place of the conventional parabolic dishes [11] with a mechanically rotating mechanism (bulky and maintenance-intensive). The recent decade has witnessed a significant boost in long-range automotive radars at 76-81 GHz [12] with a threefold increase in resolutions than the traditional 24 GHz ones [13], though costs reduction remains challenging for a wider commercialisation. As an enabler for amplitude and phase control of mm-Wave signals, LC-based phase-shifting solution has been on industrial and academic research's radar as one of the cost-effective answers for such high-accuracy-oriented beam-steering applications. A comprehensive review conducted by [14] has painted the present and past picture of LC-based microwave and mm-Wave reconfigurable devices. The chief disadvantages of LC in these frequency ranges have also been heavily exploited in the past two decades [15], among them, moderate to slow tuning speed (mainly limited by the fall time associated with the energy stored in LC) [16], and the constraint of insertion loss [17] versus the device's footprint [18] remain largely unsolved.

Nevertheless, it has continually been believed that the LC-related phase-shifting technology roadmap could navigate such challenges [15] towards scalable phased-array beam steering at mm-Wave frequencies. Repeatable voltage-controlled [19,20] and laser-driven all-optically-controlled [21,22] phase

Jinfeng Li, "Towards 76-81 GHz Scalable Phase Shifting by Folded Dual-strip Shielded Coplanar Waveguide with Liquid Crystals", *Annals of Emerging Technologies in Computing (AETiC)*, Print ISSN: 2516-0281, Online ISSN: 2516-029X, pp. 14-22, Vol. 5, No. 4, 1st October 2021, Published by International Association of Educators and Researchers (IAER), DOI: 10.33166/AETiC.2021.04.002, Available: http://aetic.theiaer.org/archive/v5/v5n4/p2.html.

shifting with continuous tuning (analogue resolution) have been experimentally verified in our previous prototypes [19-22] realised in a shielded coplanar waveguide (SCPW) configuration. Among state-of-the-art phase shifter configurations realised by LC tunable dielectrics, the main drivers for developing SCPW [19] against conventional coplanar [23,24] or single-conductor-oriented waveguide structures [25] are summarised in Table 1.

Table 1. Comparison of LC Device Structure Candidates at mm-Wave.

Topology	LC initial alignment by rubbing	Driving voltage (power consumption)	Footprint	Planarity	System integration
Waveguide	Difficult	High	Large	No	Difficult
SCPW	Ease	Low	Compact	Yes	Ease

However, there has not been much thought devoted to optimising the device's footprint, as most designs disseminated are straight-transmission-line [26] (see Figure 1 below for our demos) or straight-waveguide [25] based prototypes for proof of concept, which struggles to keep up with the miniaturisation demand [2,9]. Input to designing potentially meandered core-line structures with bespoke packaging enclosures is needed from both simulations and experiments. While classic electromagnetics [27] sheds light on perturbations of characteristic impedance and equivalent electrical length due to the bending discontinuity, no research has investigated the bending-induced perturbed dielectric volume of LC, which is closely connected with the insertion loss and phase-shifting range as well.

This work bridges the gap for miniaturisation by folding the LC-SCPW instead of using high permittivity lossy materials. Compared with straight-line designs [28], bending adds a new dimension for optimisation. Not only the PCB footprint can be reduced, but also the required LC volume may be reduced, as adjacent core lines in the meandered structure exhibit an opportunity to share a local LC volume for producing phase shifts. Note that experimentally characterising such effects would be technically demanding due to a host of non-deterministic manufacturing variables involved, such as the surface roughness [29] of conductors, multi-step treatments of the alignment layer [19], uniformity of the LC layer, etc. Fortunately, the research topic could be approached by high-fidelity simulations. The main parameter of research and optimisation interest is the dielectric volume of LC as determined by the bending structure. Given the same type of LC material at the same frequency, such an upgrade requires the effective core line length to be doubled, for which miniaturisation by bending is explored. A new meandered dual-strip SCPW structure is proposed with a proof-of-concept design at 77 GHz. A stepwise approach is followed, from the first design with a meandering core line (single-strip) for miniaturisation (as compared with the previous straight one), to a novel meandering dual-strip design.

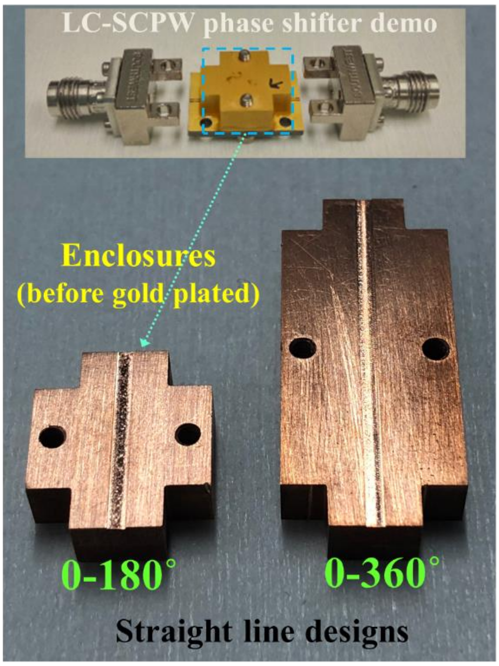

Figure 1. Demo of a straight-line LC-SCPW 0-180° continuously variable phase shifter upgrading towards a 0-360° shifting solution by doubling the effective line length

2. Single and Dual-strip Meandered SCPW Phase Shifter Designs

For the meandered two-port SCPW phase shifter design, the GT7-29001 type of LC is attempted as it exhibits the highest device's figure-of-merit (FoM) for the bespoke SCPW structure, as evidenced by our latest work [30]. The LC's dielectric constant ranges from 2.46 to 3.53, with the loss tangent ranging from 0.0064 to 0.0116 assuming negligible dispersions from 19 GHz to 77 GHz. Taconic's TLY-5A fiberglass substrate with ULPH (ultra-low-profile half oz) Cu is attempted for the non-tunable substrate material, in place of the mainstream Rogers's RT/duroid 5880 laminates with Rolled Annealed (RA) Copper. They exhibit comparable properties in the datasheet regarding dielectric, thermal (coefficient of thermal expansion), and mechanical properties (including surface roughness). The TLY-5A substrate is 0.51mm-thick, with permittivity of 2.17 and loss tangent of 0.0009 at the targeted frequency range.

As mentioned in the motivation section, one of the main deliverables of this proposal is extending the existing phase-shifting range of SCPW from the 0-180˚ by a straight line (as shown in Figure 1) towards 0-360˚. Given a same operating condition with the same device's cross-section design, such an expansion results in the length of the core line to be doubled (as illustrated in the bottom right of Figure 1 for our fabricated demo), for which meandering is necessary for miniaturisation. In recognition of the phase shift-insertion loss non-linearity, it will be interesting to see if the insertion loss of a folded design could be less than double of the existing 0-180˚ demo or not. The cross-sectional design of the single-strip folded shielded CPW (FS-CPW) is similar to that of the straight SCPW we fabricated [31].

Concerning cost reductions, a scarcity of integration on the LC materials' cost saving is well worth pondering. Particularly for mass production, the required usage (volume) of LC per device could tip the balance in the budget. Reasonably reducing the LC volume towards minimal redundancy is proposed in this work with a dual-strip FS-CPW design. Because insertion loss is largely attributed to the dielectric volumetric loss in the LC [19,26], a decreased LC volume is instrumental for reducing the dielectric loss and hence the insertion loss. Furthermore, the folded dual core-line configuration allows the enclosure for the entire LC layer to be a lump cavity, i.e., without the need for machining a meandered cavity. This modular solution means improved reconfigurability, and reasonable reduction in complexity and costs, because one type of enclosure is compatible with diverse core-line configurations.

Limitations do remain to be seen, as the bending could give rise to elevated radiation losses as well as degraded tunability (due to changing mm-Wave field directions at the bend with regard to the fixed mechanically anchoring alignment direction). The trade-off between the added bending losses (mismatching, radiation, etc.) versus the reduced LC volumetric loss is investigated for the first time in this work.

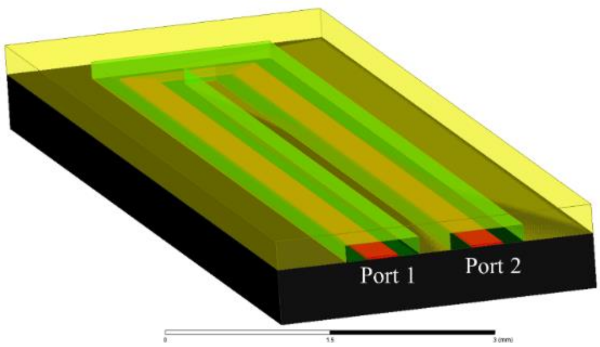

Figure 2. Geometry sketch of a meandered single-strip LC-FS-CPW (design 1)

Two designs of similar LC-FS-CPW geometries yet different modes are proposed, modelled, and compared, as schematically sketched in Figures. 2 and 3 (core line depicted in red, grounding enclosure in yellow, and filled LC in green). Both designs aim for a maximum phase shift of 360˚, while differing only on the grounding enclosure's inner arrangement. The core-line width is determined by the necessity to match the characteristic impedance. In Figure 2, port 1 (input) and port 2 (output) are separated by the enclosure's metal bar in the middle, making the two ports electromagnetically decoupled. Note that the phase shifter device is in principle reciprocal, i.e., port 2 could be treated as input and port 1 as output accordingly. In Figure 3 with the middle bar removed, both terminals share the same LC layer, resulting in a new dual-strip FS-CPW geometry. Both models are based on a uniform core line without connectorsinterfaced tapers. Tetrahedral meshing is self-adapted, with finer meshes tailored for local bending sections (with higher field gradients), and coarser meshes applied for straight-line regions.

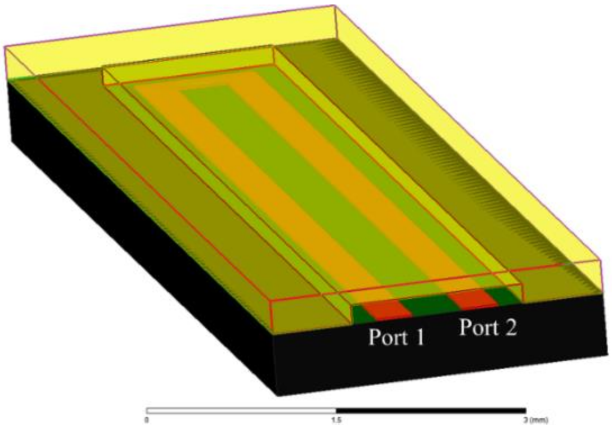

Figure 3. Geometry sketch of a novel meandered dual-strip LC-FS-CPW (design 2)

3. Computational Modelling Results and Discussion

Ansys HFSS (high-frequency structure simulator) is used as the main solver for key performance items quantified, including insertion loss and the total volume of LC at the central frequency of 77 GHz, as well as the wide-band performance (insertion loss and return loss) across 76-81 GHz.

Firstly, Figure 4 compares the dimensions for both configurations achieving the targeted 0-360° phase-shifting functionality, as well as the maximum insertion loss (minimum S_{21}). Note that the LC volume refers to the total volume of the main cavity layer (140 μm-thick defined by the enclosure wall) plus the two thin coplanar channels (depth of 17 μm as per the Cu electrode thickness).

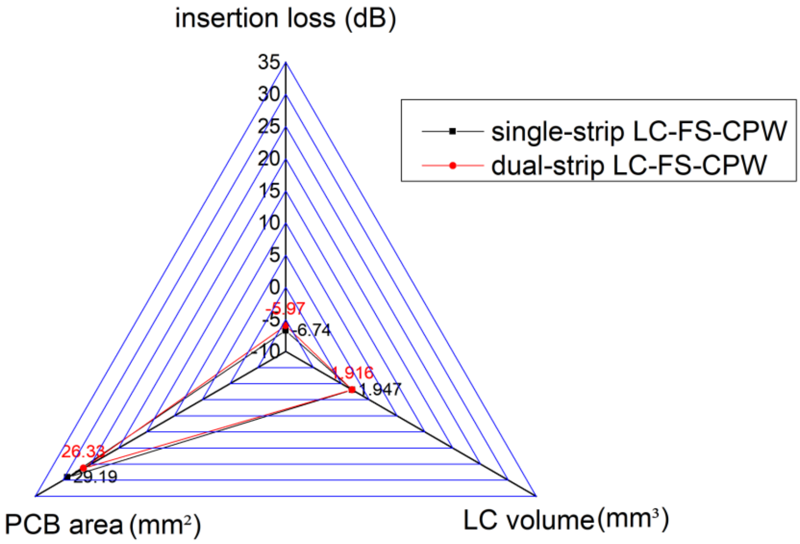

Figure 4. Performance comparison of single-strip versus dual-strip designs of LC-FS-CPW phase shifters at 77 GHz (both exhibiting a phase-shift range of 0-360°)

From the radar chart in Figure 4 above, the new dual-strip FS-CPW structure reduces the insertion loss (of single-strip one) from -6.74 dB to -5.97 dB, with the LC volume decreased by 0.031 mm³ (1.62% by volume) per device. Albeit not a noticeable change for a single device or a small-scale array (such as 4-element patch arrays [32,33]), it can result in a significant cutting of material costs for mass production in feeding a large phased-array antenna encompassing hundreds [34] if not thousands [35] of radiating elements targeting an ultra-high beam accuracy.

As observed from pie charts in Figure 5, sources of insertion loss are decomposed based on field calculations with HFSS, quantifying the power dissipation by material absorptions (dielectrics, conductors), reflection, and radiation. First, the dielectric loss in Taconic's TLY-5A substrate is infinitesimally small (0.68% of the input power) to make a difference. Comparing design 2 (dual-strip) against design 1 (single-strip), the decreased LC volume accounts for a 0.5% reduction in the LC dielectric loss, albeit radiation and crosstalk losses increase by 5%.

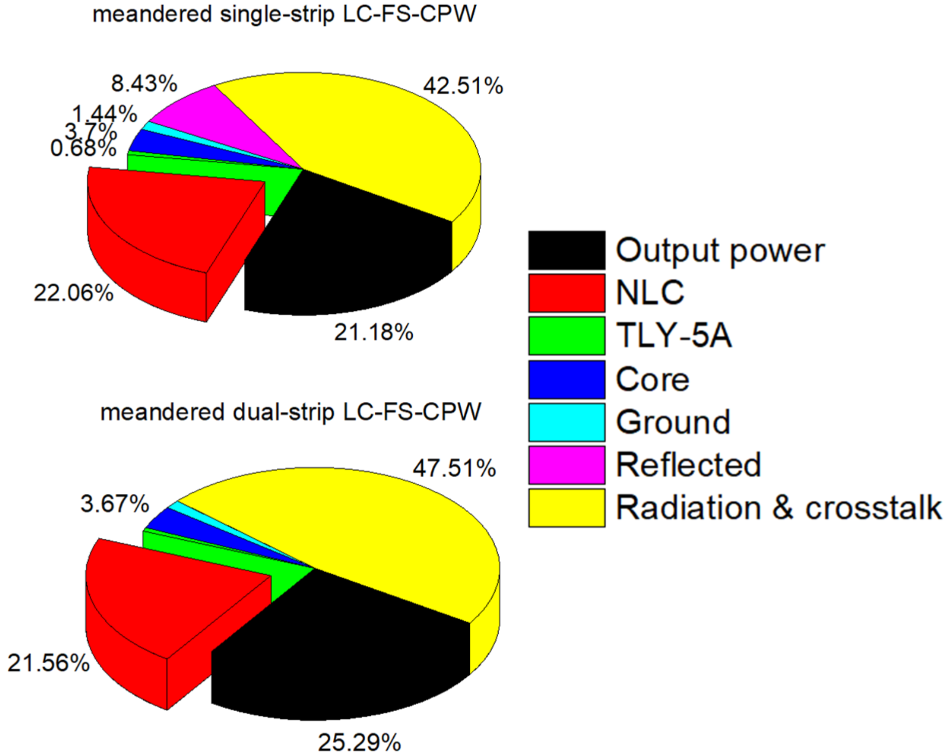

Figure 5. Power dissipation analysis of two designs at 77 GHz (input power assuming 100%)

The elevated radiation and crosstalk observed from Figure 5 (design 2 as compared with design 1) are evidenced and graphically represented in Figure 7 (design 2) as compared with Figure 6 (design 1), respectively, where the electric field intensity (V/m) is quantified on right-angled bending corners of both designs. It is worth noting the difference in the color scale bar between Figures 6 and 7, i.e., the peaking value of the electric field intensity is reduced by 16% for design 2 as compared with design 1, the results of which also agree with the reduced dielectric and metal losses shown above in Figure 5.

Regarding limitations of the designs, radiation loss dominates among the insertion loss sources (for both designs) according to Figure 5. Ongoing optimisation work will thereby centre accordingly upon the following two regimes prior to fabrication. First, mitigating radiation by means of mitered or rounded bends, and second, coupling independently by core line spacing, whilst maintaining the advantage of the shared LC layer for facilitating compact and modular phase shifters integration with each array element.

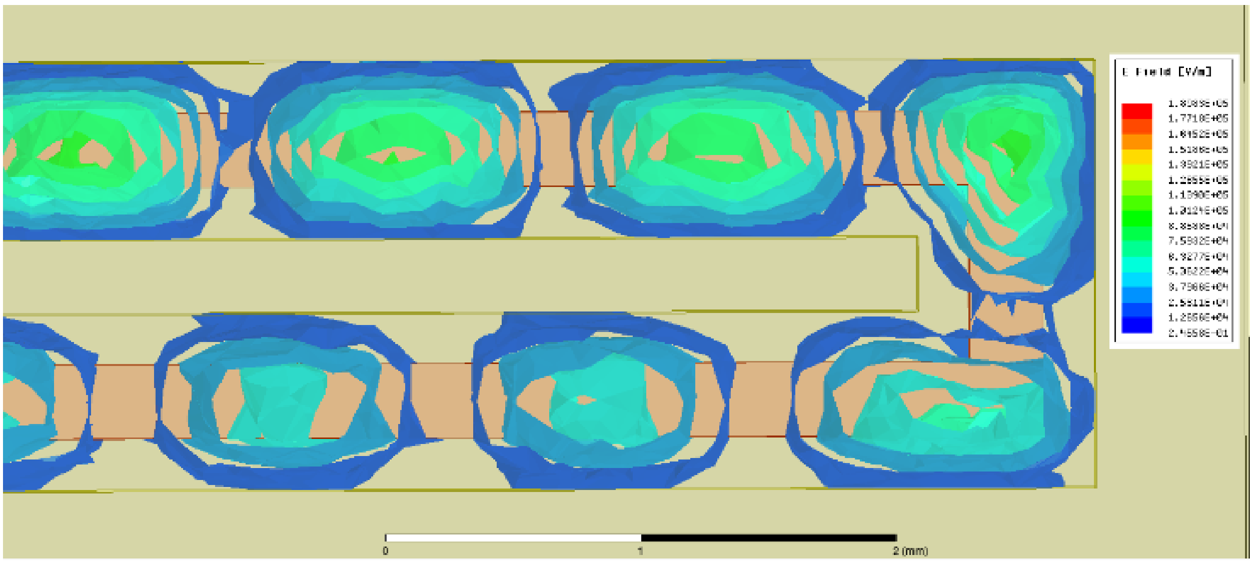

Figure 6. Electric field intensity of the LC layer in a meandered LC-FS-CPW (design 1, phase=0, zooming in the bend, top view)

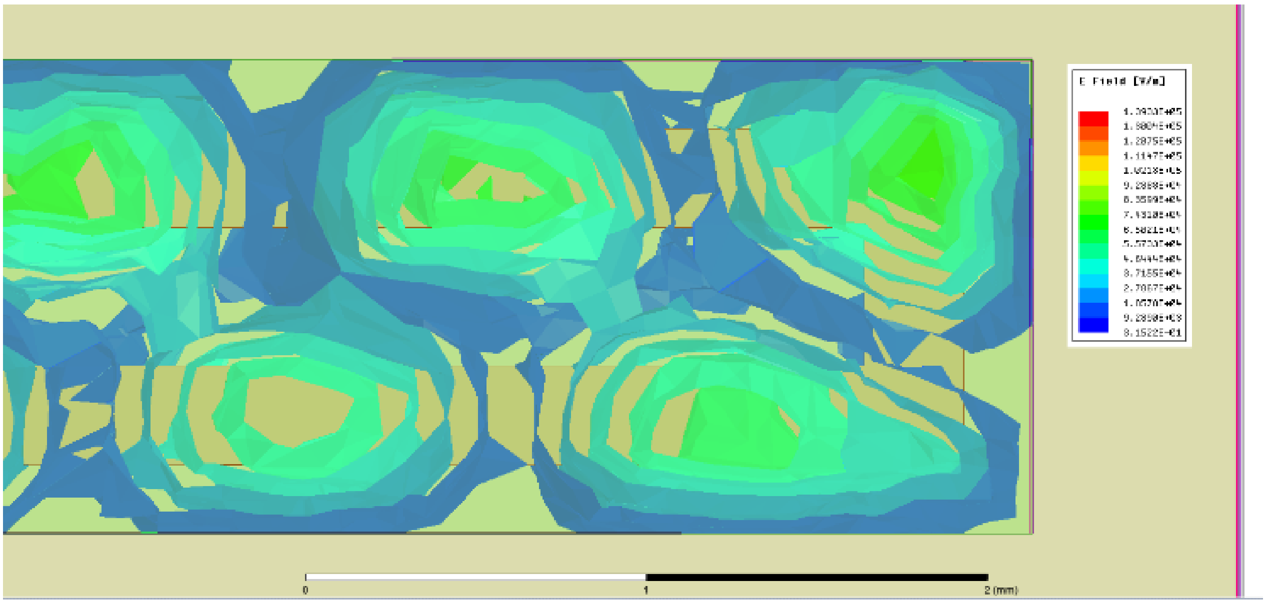

Figure 7. Electric field intensity of the LC layer in a meandered dual-strip LC-FS-CPW (design 2, phase=0, zooming in the bend, top view)

The macroscopic performance results across the spectrum of 76-81 GHz are shown in Figure 8 below for the insertion loss (IL), and Figure 9 for return loss (RL). Both maximum (max.) and minimum (min.) values of IL are presented, corresponding to the LC directors at the perpendicular and parallel state (with respect to the mm-Wave field), respectively. As evidenced in Figure 9, design 2 (the dual-strip one with the LC layer unified) is far better impedance-matched (i.e., less reflection loss) across the entire 76-81 GHz band, in particular a reflection loss as low as -38 dB is reported at the targeting central frequency of 77 GHz. The results will agree with the loss decomposition analysis reported in Figure 5.

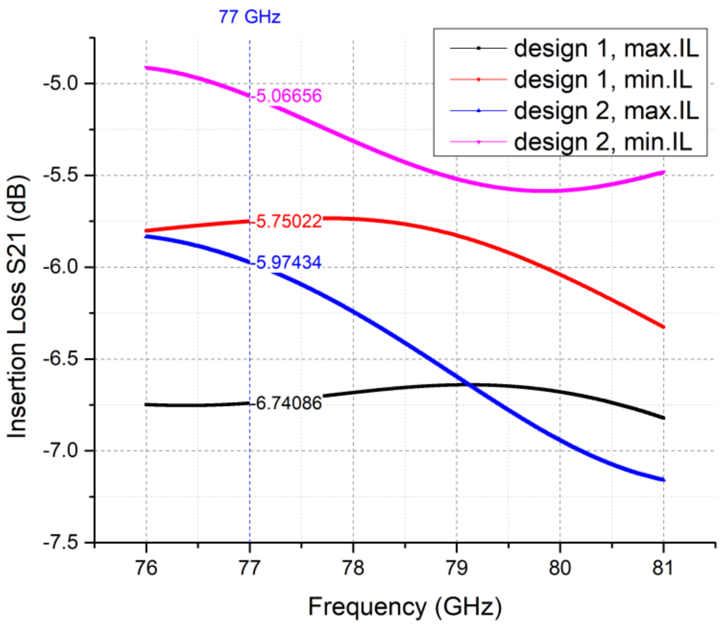

Figure 8. Insertion loss comparison between meandered single-strip (design 1) vs. dual-strip (design 2) LC-FS-CPW phase shifters

While this work focuses on insertion loss analysis of the meandered LC-FS-CPW under the targeted phase shift of 360˚, future work will quantify different bending scenarios (e.g., chamfered bend) on linearity of the phase shift as a function of driving voltages. Another scope is optimising the LC-FS-CPW phase shifter device's figure-of-merit (i.e., the ratio of the maximum differential phase shift to the maximum insertion loss) by incorporating the latest observations from [36]. Last but not least, the FS-CPW proposed is envisaged to be versatile and expandable by folding more turns to allow the LC volume to decrease more, i.e., further mitigation of insertion loss is possible.

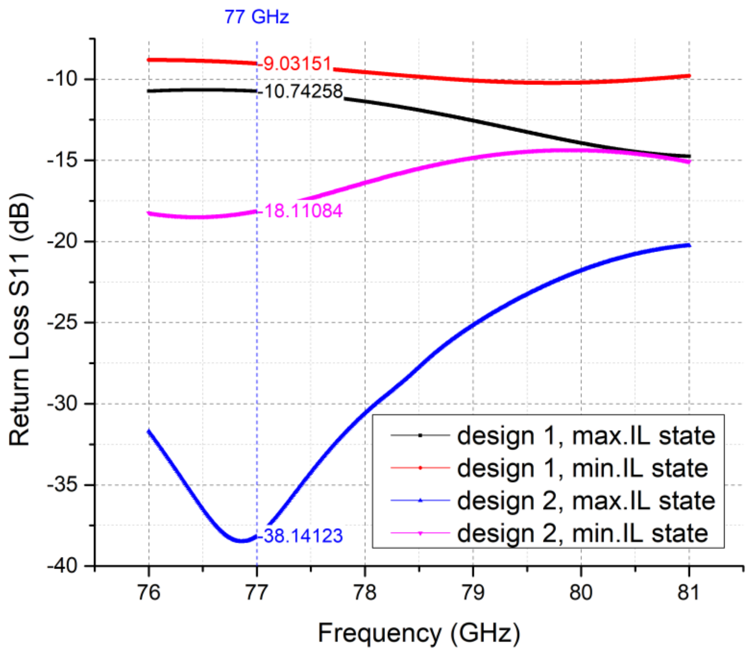

Figure 9. Return loss comparison between meandered single-strip (design 1) vs. dual-strip (design 2) LC-FS-CPW phase shifters

4. Conclusion

To support the continually multiplying applications in LC mm-Wave devices and systems, this feasibility study unlocks the miniaturisation of state-of-the-art CPW phase shifters by proposing a folded dual-strip shielded CPW (FS-CPW) mock-up for 76-81 GHz, instead of a single-strip design. As evidenced by the loss-decomposition analysis, the required LC volume and dielectric loss are both reduced for material costs saving. Particularly, the LC volume is reduced by 1.62% per device, an indication of substantial material costs saving for large antenna arrays. The forward transmission S_{21} improves from -6.74 dB to -5.97 dB, i.e., an appreciable mitigation of insertion loss, which is less than double of the 0-180° design. Another advantage lies in the modular enclosure that could be flexibly applied for different core line configurations, with significantly reduced costs for mass production, and cost-effective integration with beam-steering antennas arrays. The configuration also helps pave the way to improve enormous varieties of components and devices, e.g., filters [37], resonators, impedance adapters [20], and couplers. Nevertheless, there remains a lot of work on a shorter latency to enable car radar applications [38] and hence to make this competitive in the current industry landscape.

Acknowledgement

For the latest computational development in this work (2020-2021), the author acknowledges the University of Southampton for the supply of ANSYS Electronics Desktop (with HFSS included) as the key software for this study. The author also thanks the University of Cambridge for the underpinning early-research skills training (2014-2017) on liquid crystals passive devices for tunable radio-frequency applications. The author confirms that the computational research conducted in this work receives no external funding. The author has no conflicts of interest to declare.

References

[1] Farooq Khan and Zhouyue Pi, "mmWave mobile broadband (MMB): Unleashing the 3–300GHz spectrum", in *Proceedings of the 34th IEEE Sarnoff Symposium*, 2011, pp. 1-6, DOI: 10.1109/SARNOF.2011.5876482, Available: https://ieeexplore.ieee.org/document/5876482.

[2] JunHwan Lee, Youngseog Song, Eunyoung Choi and Juho Park "mmWave cellular mobile communication for Giga Korea 5G project", in *Proceedings of the 2015 Asia-Pacific Conference on Communications (APCC)*, Kyoto, Japan, 14–16 October 2015, DOI: 10.1109/APCC.2015.7412507, Available: https://ieeexplore.ieee.org/document/7412507.

[3] Ashraf Ali and Andrew Ware, "Effective Performance Metrics for Multimedia Mission-critical Communication Systems", *Annals of Emerging Technologies in Computing (AETiC)*, Print ISSN: 2516-0281, Online ISSN: 2516-029X,

pp. 1-14, Vol. 5, No. 2, 1st April 2021, Published by International Association of Educators and Researchers (IAER), DOI: 10.33166/AETiC.2021.02.001, Available: http://aetic.theiaer.org/archive/v5/v5n2/p1.html.

[4] Mahdi H. Miraz and Maaruf Ali, "Integration of Blockchain and IoT: An Enhanced Security Perspective", *Annals of Emerging Technologies in Computing (AETiC)*, Print ISSN: 2516-0281, Online ISSN: 2516-029X, pp. 52-63, Vol. 4, No. 4, 1st October 2020, Published by International Association of Educators and Researchers (IAER), DOI: 10.33166/AETiC.2020.04.006, Available: http://aetic.theiaer.org/archive/v4/v4n4/p6.html.

[5] Huang Xu, Cheena Hasnain, Thomas Abin and Joseph K. P. Tsoi, "Indoor Detection and Tracking of People Using mmWave Sensor", *Journal of Sensors*, vol. 2021, Article ID 6657709, 14 pages, 2021, DOI: 10.1155/2021/6657709, Available: https://www.hindawi.com/journals/js/2021/6657709/.

[6] Ogheneochuko Ubrurhe, Nigel Houlden and Peter S. Excell, "A Review of Energy Efficiency in Wireless Body Area/Sensor Networks, With Emphasis on MAC Protocol", *Annals of Emerging Technologies in Computing (AETiC)*, Print ISSN: 2516-0281, Online ISSN: 2516-029X, pp. 1-7, Vol. 4, No. 1, 1st January 2020, Published by International Association of Educators and Researchers (IAER), DOI: 10.33166/AETiC.2020.01.001, Available: http://aetic.theiaer.org/archive/v4/v4n1/p1.html.

[7] Toshiaki Nose, Ryota Ito and Michinori Honma, "Potential of Liquid-Crystal Materials for Millimeter-Wave Application", *Applied Science*, Vol. 8, No. 12, 2018, 2544, DOI: 10.3390/app8122544, Available: https://www.mdpi.com/2076-3417/8/12/2544.

[8] Jinfeng Li, "Low-loss tunable dielectrics for millimeter-wave phase shifter: from material modelling to device prototyping", in *Proceedings of the IOP Conference Series: Materials Science and Engineering*, vol. 892, 012057, 2020. DOI: 10.1088/1757-899x/892/1/012057, Available: https://iopscience.iop.org/article/10.1088/1757-899X/892/1/012057.

[9] Rolf Jakoby, Alexander Gaebler and Christian Weickhmann, "Microwave Liquid Crystal Enabling Technology for Electronically Steerable Antennas in SATCOM and 5G Millimeter-Wave Systems", *Crystals*, Vol. 10, No. 5, 514, 2020, DOI: 10.3390/cryst10060514, Available: https://www.mdpi.com/2073-4352/10/6/514.

[10] Pat Hindle, "Comprehensive Survey of Commercial mmWave Phased Array Companies Focused on SATCOM and 5G Applications", *Microwave Journal*, 2020. Available: https://www.microwavejournal.com/articles/33357-comprehensive-survey-of-commercial-mmwave-phased-array-companies

[11] Bin Deng, Hong-Qiang Wang, Yu-Liang Qin, Sha Zhu and Xiang Li, "Rotating Parabolic-Reflector Antenna Target in SAR Data: Model, Characteristics, and Parameter Estimation", *International Journal of Antennas and Propagation*, vol. 2013, Article ID 583865, 2013, DOI: 10.1155/2013/583865, Available: https://www.hindawi.com/journals/ijap/2013/583865/.

[12] Frank Sickinger, Ernst Weissbrodt and Martin Vossiek, "76–81 GHz LTCC antenna for an automotive miniature radar frontend", in *Proceedings of the 2017 European Radar Conference (EURAD)*, pp. 374-377, 2017, DOI: 10.23919/EURAD.2017.8249225, Available: https://ieeexplore.ieee.org/document/8249225.

[13] M. Klotz and H. Rohling, "24 GHz radar sensors for automotive applications", in *13th International Conference on Microwaves, Radar and Wireless Communications. MIKON - 2000*, pp. 359-362 vol. 1, 2000, DOI: 10.1109/MIKON.2000.913944, Available: https://ieeexplore.ieee.org/document/913944.

[14] Holger Maune, Matthias Jost, Roland Reese, Ersin Polat, Matthias Nickel and Rolf Jakoby, "Microwave Liquid Crystal Technology", *Crystals*, Vol. 8, No. 9, 355, 2018, DOI: 10.3390/cryst8090355, Available: https://www.mdpi.com/2073-4352/8/9/355.

[15] Jinfeng Li, "Performance Limits of Liquid Crystals Coplanar Phase Shifters beyond 60 GHz due to Fabrication", in *Proceedings of the IEEE International Conference on Computing, Networking, Telecommunications & Engineering Sciences Applications*, Tirana, Albania, 2020, pp. 21-26. DOI: 10.1109/CoNTESA50436.2020.9302865, Available: https://ieeexplore.ieee.org/document/9302865.

[16] Dimitrios C. Zografopoulos & Romeo Beccherelli, "Tunable terahertz fishnet metamaterials based on thin nematic liquid crystal layers for fast switching", *Scientific Reports*, Vol. 5, 13137, 2015, DOI: 10.1038/srep13137, Available: https://www.nature.com/articles/srep13137.

[17] Toshiaki Nose, Tomoya Ito, Ryota Ito and Michinori Honma, "Basic Performance of Rectangular Waveguide Type Liquid Crystal Phase Shifter Driven by Magnetic Field", in *43rd International Conference on Infrared, Millimeter, and Terahertz Waves*, Nagoya, Japan, 2018, pp. 1-2, DOI: 10.1109/IRMMW-THz.2018.8510116, Available: https://ieeexplore.ieee.org/document/8510116.

[18] Jinfeng Li, "Bias Tees Integrated Liquid Crystals Inverted Microstrip Phase Shifter for Phased Array Feeds", in *21st International Conference on Electronic Packaging Technology*, Guangzhou, pp. 1-5, 2020, DOI: 10.1109/ICEPT50128.2020.9202604, Available: https://ieeexplore.ieee.org/document/9202604.

[19] Jinfeng Li and Daping Chu, "Liquid crystal-based enclosed coplanar waveguide phase shifter for 54–66 GHz applications", *Crystals*, Vol. 9, No. 12, 650, December 2019, DOI: 10.3390/cryst9120650, Available: https://www.mdpi.com/2073-4352/9/12/650.

[20] Jinfeng Li, "Wideband PCB-to-Connectors Impedance Adapters for Liquid Crystal-Based Low-Loss Phase Shifters", in *50th European Microwave Conference*, Utrecht, Netherlands, pp. 546-549, 2021, DOI: 10.23919/EuMC48046.2021.9337967, Available: https://ieeexplore.ieee.org/document/9337967.

[21] Jinfeng Li, "All-optically Controlled Microwave Analog Phase Shifter with Insertion Losses Balancing", *Engineering Letters*, vol. 28, no. 3, pp. 663-667, 2020, Available: http://www.engineeringletters.com/issues_v28/issue_3/EL_28_3_03.pdf.

[22] Jinfeng Li, "Optically Steerable Phased Array Enabling Technology Based on Mesogenic Azobenzene Liquid Crystals for Starlink Towards 6G", in *2020 IEEE Asia-Pacific Microwave Conference (APMC)*, Hong Kong, 2020, pp. 345-347, DOI: 10.1109/APMC47863.2020.9331345, Available: https://ieeexplore.ieee.org/document/9331345.

[23] Rainee N. Simons, "Conductor Backed Coplanar Waveguide", in *Coplanar Waveguide Circuits, Components, and Systems*, IEEE, 2001, pp.87-111, DOI: 10.1002/0471224758.ch3.

[24] Rainee N. Simons, "Coplanar Waveguide with Finite-Width Ground Planes", in *Coplanar Waveguide Circuits, Components, and Systems*, IEEE, 2001, pp.112-126, DOI: 10.1002/0471224758.ch4.

[25] Roland Reese, Ersin Polat, Henning Tesmer, Jonathan Strobl, Christian Schuster *et al.*, "Liquid Crystal Based Dielectric Waveguide Phase Shifters for Phased Arrays at W-Band", *IEEE Access*, vol. 7, pp. 127032-127041, 2019, DOI: 10.1109/ACCESS.2019.2939648, Available: https://ieeexplore.ieee.org/document/8825834.

[26] Jinfeng Li, Huan Xu and Daping Chu, "Design of liquid crystal based coplanar waveguide tunable phase shifter with no floating electrodes for 60–90 GHz applications", in *46th European Microwave Conference*, London, 2016, pp. 1047-1050, DOI: 10.1109/EuMC.2016.7824526, Available: https://ieeexplore.ieee.org/document/7824526.

[27] Lin W., Cheng Y. and Wang R., "A New Theory of Calculating Bending Radiation Losses", *Journal of Electromagnetic Waves and Applications*, 1991, 5:11, pp. 1187-1198, DOI: 10.1163/156939391X00789.

[28] Jinfeng Li, "Millimetre-wave beam steering with analog-resolution and minimised distortion based on liquid crystals tunable delay lines with enhanced signal-to-noise ratios", in *Proceedings of the Millimetre Wave and Terahertz Sensors and Technology XIII*, vol. 11541, 115410H, September 2020, DOI: 10.1117/12.2570001.

[29] Jinfeng Li, "60 GHz Optimised Nickel-free Gold-plated Enclosed Coplanar Waveguide Liquid Crystal Phase Shifter", in *IEEE MTT-S International Microwave Workshop Series on Advanced Materials and Processes for RF and THz Applications*, Suzhou, China, 2020, pp. 1-3, DOI: 10.1109/IMWS-AMP49156.2020.9199680.

[30] Jinfeng Li, "Figure-of-Merits Mismatch in Liquid Crystals mmWave Phase Shifters", in *Proceedings of the 46th International Conference on Infrared, Millimeter, and Terahertz Waves*, Chengdu, China, 2021.

[31] Jinfeng Li, "An Efficient Mixed-signal Dielectric-partitioning Model of Liquid Crystals based Shielded Coplanar Waveguide for Electronically Reconfigurable Delay Lines Design", in *Proceedings of the Integrated Optics: Design, Devices, Systems and Applications VI*, vol. 11775, 1177519, April 2021, DOI: 10.1117/12.2593624.

[32] Prafulla Deo, Dariush Mirshekar-Syahkal, Lawrence Seddon, Sally E. Day and F. Aníbal Fernández, "Liquid crystal based patch antenna array for 60 GHz applications", in *2013 IEEE Radio and Wireless Symposium*, 2013, pp. 127-129, DOI: 10.1109/RWS.2013.6486663, Available: https://ieeexplore.ieee.org/document/6486663.

[33] Aydin Babakhani, Xiang Guan, Abbas Komijani, Arun Natarajan and Ali Hajimiri, "A 77-GHz Phased-Array Transceiver with On-Chip Antennas in Silicon: Receiver and Antennas", *IEEE Journal of Solid-State Circuits*, Vol. 41, No. 12, pp. 2795-2806, 2006, DOI: 10.1109/JSSC.2006.884811.

[34] Umut Kodak, Bhaskara Rupakula, Samet Zihir and Gabriel M. Rebeiz, "60-GHz 64- and 256-Element Dual-Polarized Dual-Beam Wafer-Scale Phased-Array Transceivers with Reticle-to-Reticle Stitching", *IEEE Transactions on Microwave Theory and Techniques*, Vol. 68, No. 7, pp. 2745-2767, July 2020, DOI: 10.1109/TMTT.2020.2969904.

[35] Larry Corey, Esko Jaska and Joseph Guerci, "Phased-array development at DARPA", in *IEEE International Symposium on Phased Array Systems and Technology*, Boston, USA, 2003, pp. 9-16, DOI: 10.1109/PAST.2003.1256949.

[36] Jinfeng Li, "Rethinking Figure-of-Merits of Liquid Crystals Shielded Coplanar Waveguide Phase Shifters at 60 GHz", *J*, Vol. 4, No. 3, pp. 444-451, August 2021, DOI: 10.3390/j4030034, Available: https://www.mdpi.com/2571-8800/4/3/34.

[37] Mani Yazdanpanahi, Prafulla Deo and Dariush Mirshekar-Syahkal, "Tunable liquid-crystal millimeter-wave bandpass filter using periodical structure", in *IEEE Radio and Wireless Symposium (RWS)*, Newport Beach, USA, 2014, pp. 163-165, DOI: 10.1109/RWS.2014.6830078, Available: https://ieeexplore.ieee.org/document/6830078.

[38] Mehdi SeyyedEsfahlan, Efe Öztürk, Mehmet Kaynak and Ibrahim Tekin, "77-GHz Four-Element Phased-Array Radar Receiver Front End", in *IEEE Transactions on Components, Packaging and Manufacturing Technology*, Vol. 6, No. 8, pp. 1162-1173, 15 June 2016, IEEE, DOI: 10.1109/TCPMT.2016.2571742, Available: https://ieeexplore.ieee.org/document/7492207.